

Black Holes in General Relativity and Beyond [†]

Enrico Barausse ^{1,2,3}

¹ Institut d'Astrophysique de Paris, CNRS & Sorbonne Universités, UMR 7095, 98 bis bd Arago, 75014 Paris, France; barausse@sissa.it

² SISSA, Via Bonomea 265, 34136 Trieste, Italy

³ IFPU—Institute for Fundamental Physics of the Universe, Via Beirut 2, 34014 Trieste, Italy

[†] Presented at the Recent Progress in Relativistic Astrophysics, Shanghai, China, 6–8 May 2019.

Published: 14 June 2019



Abstract: The recent detections of gravitational waves from binary systems of black holes are in remarkable agreement with the predictions of General Relativity. In this pedagogical mini-review, I go through the physics of the different phases of the evolution of black hole binary systems, providing a qualitative physical interpretation of each one of them. I also briefly describe how these phases would be modified if gravitation were described by a theory extending or deforming General Relativity, or if the binary components turned out to be more exotic compact objects than black holes.

1. Introduction

The binary black hole (BH) systems detected by ground based gravitational wave (GW) interferometers (first by the two LIGOs alone [1–5], then by the LIGO–Virgo network [6,7]) are now ten, and their signals have been found to be in excellent agreement with the predictions of General Relativity (GR). While GR had previously passed experimental tests with flying colors in weak field and/or mildly relativistic regimes (in the solar system [8] and in binary pulsars [9,10]), the LIGO–Virgo detections provide for the first time evidence that GR is viable in the strong gravity, highly relativistic and dynamical regime relevant for BH binaries [3,11]. Moreover, they also support the hypothesis that the binary's components, as well as the merger remnant, are really BHs, as opposed to more exotic compact objects [1].

Nevertheless, as always in physics, these statements on the correctness of GR and on the BH hypothesis come with several caveats, and they are only correct within the “experimental errors” affecting the measurements. In other words, while large non-perturbative effects in the GW signal seem to be ruled out by current observations [3,11], deformations of the general relativistic signal that are either sufficiently small and/or in the frequency ranges where LIGO and Virgo are least (or not at all) sensitive may still be in agreement with observations.

The purpose of this note is to briefly scope out where deviations from GR or from the BH hypothesis might still hide in the GW signal from binary systems, while remaining in agreement with observations. I do so by conventionally splitting the signal into four parts: an early low-frequency portion produced by the binary's inspiral (Section 2); one produced by the merger (Section 3) with the subsequent ringdown phase (Section 4); and a post-ringdown phase produced by putative exotic near horizon physics (Section 6). (This fourth phase is of course absent in GR.) I qualitatively interpret each part by relying on physical intuition from the test particle limit, Newtonian physics and BH perturbation theory.

2. The Inspiral

At low orbital (and GW) frequencies, i.e., at large separations, the evolution of the binary is driven by the emission of GWs. The latter backreact on the system by carrying energy and angular momentum

away from it, and thus cause the binary to slowly inspiral to smaller and smaller separations. In GR, this “(gravitational) radiation reaction” is well described, in the limit of small relative binary velocities $v \ll c$, by the quadrupole flux formula, according to which the energy flux emitted by a binary with masses m_1 and m_2 and separation r is given by [12]

$$\dot{E}_{\text{quadrupole}} = \frac{32G}{5c^3} \left(\frac{Gm_1m_2}{r^2} \right)^2 \left(\frac{v}{c} \right)^2. \quad (1)$$

For a quasi-circular binary, Kepler’s law yields $v = (GM/r)^{1/2}$ (with $M = m_1 + m_2$), and the GW frequency f is given by twice the orbital frequency $f_{\text{orb}} = v/(2\pi r)$. One can then relate the GW frequency to the binary’s total energy E (in the center of mass frame) by $E = -Gm_1m_2/(2r)$, and re-express Equation (1) as [12]

$$\dot{f} = \frac{96G^{5/3}}{5c^5} \pi^{8/3} \mathcal{M}^{5/3} f^{11/3}, \quad (2)$$

where $\mathcal{M} = Mv^{3/5}$, with $v = m_1m_2/M^2 \leq 1/4$, is the *chirp mass*. A simple lesson to be drawn from this equation is that GW observations of the inspiral determine the chirp mass to high accuracy, simply by measuring the frequency and its rate of change. Indeed, the first GW detection (GW150914 [1]) determined the chirp mass of the binary source to be $\mathcal{M} \approx 30M_\odot$, which translates into a total mass $M \gtrsim 70M_\odot$.

The quadrupole formula can be generalized by performing a “post-Newtonian” (PN) expansion, i.e., a perturbative expansion of the field equations in the small quantity $v/c \ll 1$ (see, e.g., Ref. [13] for a review of the PN formalism). By solving the field equations under that approximation, one can find expressions for the fluxes that reduce to Equation (1) in the limit of low frequencies (when $v \ll c$), but which also include subdominant terms in v/c (e.g., the mass-octupole and current-quadrupole contributions). These terms become important as the binary’s separation shrinks. Similar PN-expanded expressions can be found not only for the GW fluxes, but also for the gravitational waveforms and for the Hamiltonian describing the conservative interaction between the two binary components.

In particular, the PN expansion allows one to account for the effect of BH spins, which appear in both the conservative and dissipative sectors. One remarkable effect of BH spins during the inspiral is given by the modulations of the GW amplitude that they cause when they are misaligned with the binary’s orbital angular momentum [14]. Indeed, save for special configurations giving rise to *transitional precession* [14], the spins and the orbital angular momentum undergo *simple precession* around the total angular momentum of the system, whose direction remains approximately constant during the binary’s evolution (including even the merger ringdown phase) [14,15]. Detecting these spin precession modulations, as well other spin related effects in the gravitational waveforms (e.g., the dependence of the plunge-merger frequency on the spins, which we will discuss below in Section 3, and the enhancement of the GW amplitude caused by large spins aligned with the orbital angular momentum), one can, at least in principle, measure BH spins. Indeed, in two GW detections (GW151226 and GW170729) there seems to be evidence in favor of non-zero, probably precessing spins [2,3,7]. Much more accurate measurements of BH spins (to within 1–10% or better) will also become possible with space based detectors such as LISA [16,17].

As one moves away from GR to consider more general gravitational theories, the structure of the PN expansion also gets modified. The LIGO-Virgo collaboration has performed phenomenological tests of GR by “deforming” the PN expressions for the GW amplitude and phase as functions of frequency. In particular, they allowed for PN coefficients (i.e., coefficients akin, e.g., to the $32/5$ appearing in Equation (1)) different from the GR predicted values, and tried to constrain the differences away from the latter with observations. This resulted in “large” deviations from GR being excluded by the data [3,11]. Note that these deformations of the PN coefficients may effectively account also for the possibility that the binary components may not be BHs but more exotic objects, which would present different tidal effects than BHs (see, e.g., Ref. [18]).

Another effect that would arise quite naturally from an extension/modification of GR is a low-frequency change of the fluxes and waveforms, resulting e.g., from the existence of BH dipole radiation [19]. Within GR, gravitational monopole and dipole radiation are forbidden by the conservation of the stress energy tensor, i.e., respectively, by the conservation of energy and linear momentum. This is similar to what happens in electromagnetism, where monopole emission is forbidden by the conservation of the electric charge. Suppose now, however, that the theory of gravity describing Nature is not GR (which only possesses a spin-2 graviton, i.e., which only describes gravity by means of a metric), but some more general theory in which gravity is described by a metric *and* additional gravitational degrees of freedom (e.g., a scalar field). To avoid the appearance of unwanted fifth forces in existing experiments, these additional gravitons must be coupled very weakly (if they are coupled at all) to matter, but they may be coupled non-minimally to the metric. As a result, the coupling to matter, which is negligible in weak gravity experiments such as those performed on Earth, may re-appear in strong gravity systems, where non-linearities of the metric become large enough to mediate an effective coupling between matter and the extra gravitational fields.

One may parameterize this effective coupling (also known as “Nordtvedt effect” [20–22]) by “charges” carried by compact objects such as BHs and neutron stars. These charges, also referred to as “sensitivities” [20,23–28], can be object-dependent, e.g., they can be different for BHs and neutron stars, or for stars of different compactness (as they need to vanish in the small compactness limit, i.e. they are negligible for stars or objects with weak internal gravity). In this sense, they may be viewed also as parameterizing violations of the universality of free fall (the equivalence principle). The latter holds in GR, but is generally violated beyond GR, at least in strong field regimes, because of energy and momentum exchanges between matter and the extra gravitational degrees of freedom, mediated by the large metric perturbations.

Now, just as in Maxwell’s theory a binary system of objects carrying unequal electric charges emits dipole radiation, a quasi-circular binary of BHs or neutron stars carrying unequal sensitivities $s_1 \neq s_2$ will emit (gravitational) dipole radiation. Such an emission would be enhanced relative to the quadrupole flux of Equation (1) by a term $\sim (s_1 - s_2)^2 (v/c)^{-2}$, i.e., it would dominate the binary evolution at low frequencies [20,23–28].

Bounds on the existence of this dipole radiation are very strong in binary pulsar systems (see, e.g., Ref. [29]), but little can be inferred from those bounds about BH dipole emission, since sensitivities can be different for different classes of objects. Indeed, theories exist where the sensitivities are exactly zero for stars (including neutron stars), and non-zero only for BHs [30,31]. Bounds on BH dipole emission from LIGO-Virgo are rather loose, since these detectors cannot observe the low-frequency ($\lesssim 10$ Hz) signal from the early inspiral because of instrumental limitations (mainly due to seismic and Newtonian noise). However, much more stringent bounds will be made possible by the launch of the ESA-led mission LISA [16], a space-borne GW detector targeting the mHz frequency band. This will allow for observing the low frequency inspiral of LIGO-Virgo sources before they are detected from the ground [32], and also to observe massive BH binaries [17] and extreme mass ratio inspirals [33]. This will result in bounds on the BH dipole flux several orders of magnitude stronger than current ones [19].

3. The Merger

Under the effect of radiation reaction, a BH binary slowly evolves along quasi-circular orbits with decreasing separation. Unlike in Newtonian mechanics, where circular orbits can exist with arbitrarily small radii around a point mass, in GR there exists an innermost stable circular orbit (ISCO), inside which circular orbits can still exist but are unstable [34]. ISCOs do indeed exist for test particles (i.e., in the limit $m_2/m_1 \rightarrow 0$) around Schwarzschild and Kerr BHs, and they are present also away from the test particle limit, e.g., when one includes next-to-leading order corrections in $\mathcal{O}(m_2/m_1)$, or when one expands the dynamics of generic mass ratio binaries in a PN series (in the latter case, the ISCO

corresponds to the circular orbit with minimum energy, as defined by the PN Hamiltonian mentioned in the previous section) [35–37].

The position of the ISCO, its energy and its angular momentum depend on the parameters of the BH binary, and most notably on the spins. This is easily seen in the test particle limit, i.e., for the ISCO of the Kerr geometry. As the spin of the Kerr BH (projected on the direction of the particle’s orbital angular momentum) increases, the ISCO moves inwards, while its energy and angular momentum decrease [38]. In particular, the ISCO for a test particle moving on retrograde orbits (with respect to the BH rotation) in a Kerr spacetime lies at larger radii than for a particle on prograde orbits [38]. This behavior is of course a manifestation of the more general “frame dragging” effect of GR, whereby matter near BH horizons tends to co-rotate with the BH as seen from infinity. It is also the reason why the radiative efficiency of thin accretion disks, whose inner edge lies at the ISCO of the central BH, is an increasing function of the BH spin, and why their inner edge gets closer and closer to the BH as the spin of the latter increases. Both facts are crucial to estimate the spin of BH candidates by electromagnetic observations such as continuum fitting and iron-K α lines [39,40]. Similarly, any modification of the BH geometry causing an ISCO shift (as a result of a deviation of the gravity theory from GR, or simply because the central object is more exotic than a run-of-the-mill BH) can be constrained, at least in principle, by the same electromagnetic techniques [41,42].

As in the test-particle limit, the position of the effective ISCO of a comparable mass binary moves to smaller separation for larger BH spins [35,37,43]. Once the binary reaches the ISCO, it cannot transition to a stable circular orbit and therefore plunges and merges. The plunge–merger phase takes place in a dynamical time $\sim GM/c^3$, i.e., it is much shorter than the inspiral phase. For this reason, the GW fluxes emitted in the plunge–merger phase can be neglected, to first approximation, with respect to those emitted during the inspiral, i.e., most of the energy and angular momentum emitted by a BH binary is lost from large separations down to the effective ISCO of the system. Therefore, as in the case of thin accretion disks (whose radiative efficiency increases with the spin of the central BH), the GW emission efficiency of BH binaries is a growing function of the spins [44] (because larger spins imply smaller ISCO separations, and thus longer inspiral phases and larger integrated GW fluxes).

One can also attempt to estimate the final spin of the BH remnant produced by the merger that follows the plunge by conserving angular momentum. Consider for instance a test particle falling into a BH from a quasicircular equatorial inspiral. Neglecting the fluxes during the plunge–merger, and also neglecting the fraction of the binary’s mass emitted in GWs (see Ref. [45] for a treatment that avoids this second hypothesis), the final spin of the BH is

$$a_{\text{fin}} = \frac{1}{(1+q)^2} \left(a_1 + a_2 q^2 + \tilde{L}_{\text{ISCO}}(a_1) q \right), \quad (3)$$

where $q = m_2/m_1 \ll 1$ and $\tilde{L}_{\text{ISCO}}(a_1)$ is the ISCO angular momentum (normalized by Gm_1m_2/c to make it dimensionless) as a function of the central (“primary”) BH spin a_1 . Let us look for instance at the simple case of non-spinning BHs, $|a_1| = |a_2| = 0$, and extrapolate from the test-particle limit to equal masses, $q = 1$. The final predicted spin is then $a_{\text{fin}} \approx 0.866$, which is quite off compared to $a_{\text{fin}} \approx 0.686$ predicted by numerical relativity simulations of BH mergers [46]. However, if the primary BH spin a_1 used to compute \tilde{L}_{ISCO} is replaced by a_{fin} , one is left with an algebraic equation in a_{fin} , which can be solved, e.g., by iteration [47]. Remarkably, this procedure gives an excellent estimate for the final spin, $a_{\text{fin}} \approx 0.66$ [47]. This iterative method can be generalized to generic (even misaligned) spins and mass ratios, and turns out to be always in good agreement with numerical relativity simulations [45,47]. (See also Refs. [15,48–51] for other procedures to estimate the final spin based on similar physical arguments.)

At least two lessons can be drawn from this method to estimate the final spin. The first is that there seems to be a mapping between the comparable mass BH binary problem and the dynamics of a test particle in a Kerr spacetime with spin equal to the final spin. The existence of this mapping is hardly surprising because similar mappings between the comparable mass and test-particle two-body

problems are known to exist, e.g., in Newtonian mechanics (where a binary can be mapped into a test particle of mass $m_1 m_2 / M$ around a point mass $M = m_1 + m_2$), in quantum electrodynamics (where one can map the energy levels of positronium into those of hydrogen [52]) and in PN theory itself (with the effective one-body (EOB) model, applicable to the inspiral phase of non-spinning [53] and spinning [54,55] BH binaries). Indeed, the success of the iterative method in Ref. [47] to compute the final spin, which we have outlined above, provides justification for extending the EOB model through the merger ringdown phase [56].

Secondly, it should be stressed that, if deviations from GR or from the BH paradigm itself were to change the position and angular momentum of the effective ISCO of a BH binary, then Equation (3) and the “amended” extrapolation procedure in Ref. [47] would produce a different final BH spin. While direct measurements of the final spin by LIGO and Virgo are currently impossible because of the low signal-to-noise ratio (SNR) of the ringdown [11], future detectors such as LISA will allow for measurements of the ringdown with SNR of several hundreds [57], thus making direct spin measurements possible. Moreover, even with the current LIGO-Virgo detections one can attempt to perform consistency tests between the inspiral part of the waveforms (which depends on the individual masses and spins) and the plunge–merger–ringdown part (which depends on the final mass and spin). These tests provide at present no signs of large deviations away from GR [3,11] (see also the next section).

Another notable constraint on the nature of the components of the LIGO-Virgo binaries can be obtained from simple physical arguments involving the merger part of the waveform. As mentioned previously, the GW150914 BH merger event has chirp mass $\mathcal{M} \sim 30 M_\odot$ ($M \sim 70 M_\odot$), as estimated from the inspiral. The peak of the GW amplitude, corresponding to the merger, is at about 150 Hz, corresponding to an orbital frequency of ~ 75 Hz and a separation (assuming a binary with roughly equal masses) of ~ 350 km [1]. Since $GM/c^2 \sim 200$ km, this means that the components of GW150914 merge when they are very close (in gravitational radii). If they were more exotic compact objects with sizes $R_1 + R_2 \gg GM/c^2$, they would be interacting well before reaching a separation of 350 km, which would trigger an earlier merger than for BHs. This seems to disfavor the hypothesis that the binary components could be, e.g., boson stars [1], unless their compactness is very close to that of BHs (which in turns puts restrictions on the potential of the bosonic degrees of freedom). These bounds are much stronger than those for BHs in the massive/supermassive range, which come e.g., from tracking S-stars around the massive BH at the center of our Galaxy [58], and which still allow for a compactness $GM/(Rc^2) \gtrsim 10^{-3}$. Moreover, note that deviations from GR may also trigger early mergers, especially in the presence of non-perturbative effects (cf. Ref. [59,60] for an example of a theory triggering early mergers of neutron star systems).

4. The Ringdown

When the two binary components coalesce, the remnant is initially highly perturbed as a result of the violent merger process. As the system evolves toward an asymptotically stationary state, the amplitude of these perturbations decreases and eventually becomes sufficiently small for them to be described by linear theory. Within GR, linear perturbations $h_{\mu\nu}$ over a generic vacuum spacetime with metric $g_{\mu\nu}$ satisfy the wave equation [61,62]

$$\square \bar{h}^{\alpha\beta} + 2R_{\mu}^{\alpha}{}_{\nu}^{\beta} \bar{h}^{\mu\nu} = 0, \quad (4)$$

with $\bar{h}_{\mu\nu} \equiv h_{\mu\nu} - h_{\alpha}^{\alpha} g_{\mu\nu}/2$ obeying the Lorenz gauge condition $\nabla_{\nu} \bar{h}^{\mu\nu} = 0$, and $\square \equiv g^{\mu\nu} \nabla_{\mu} \nabla_{\nu}$.

However, linear perturbations over a Kerr background of gravitational radius $r_s = GM/c^2$ (M being the mass) and spin parameter $a \in [0, 1]$ are better described by the Newman–Penrose scalars [63]

$$\Psi_0 = -C_{\mu\nu\lambda\sigma} l^{\mu} m^{\nu} l^{\lambda} m^{\sigma}, \quad (5)$$

$$\Psi_4 = -C_{\mu\nu\lambda\sigma} n^{\mu} m^{*\nu} n^{\lambda} m^{*\sigma}, \quad (6)$$

where $C_{\mu\nu\lambda\sigma}$ is the Weyl curvature tensor, and l, n, m, m^* constitute a (complex) null tetrad, defined at each spacetime point. Note that Ψ_0 and Ψ_4 can be thought of as describing ingoing and outgoing GWs.

Because of the symmetries of the Kerr metric (and in particular the existence of a Killing tensor, besides the Killing vectors associated to stationarity and axisymmetry), the linear perturbation equations are dramatically simplified by a decomposition in Fourier modes and in spin-weighted spheroidal harmonics ${}_sS_{lm}$ (with $s = 2$ and $s = -2$ for Ψ_0 and Ψ_4), i.e., by adopting the ansatz [64]

$$\psi(t, r, \theta, \phi) = \frac{1}{2\pi} \int e^{-i\omega t} \sum_{l=|s|}^{\infty} \sum_{m=-l}^l e^{im\phi} {}_sS_{lm}(\theta) R_{lm}(r) d\omega, \quad (7)$$

where ψ stands for either Ψ_0 or $\rho^{-4}\Psi_4$, with $\rho \equiv -1/(r - iar_s \cos \theta)$. Indeed, with this decomposition, the perturbed field equations reduce to a single ordinary differential equation for the radial function R_{lm} [64]:

$$\Delta \partial_r^2 R_{lm} + 2(s+1)(r-r_s) \partial_r R_{lm} + V R_{lm} = 0, \quad (8)$$

with $\Delta = r^2 - 2rr_s + a^2 r_s^2$ and V a (complex) potential depending on ω, r, M, a, s, l and m . Moreover, by introducing the tortoise coordinate r_* , which ranges from $-\infty$ at the horizon to $+\infty$ at spatial infinity, one can zoom in onto the near horizon region, and the equation becomes reminiscent of the one-dimensional Schrodinger equation with a potential barrier.

This equation should be solved with boundary conditions corresponding to no radiation incoming from infinity (i.e., the system is isolated) and no radiation exiting the event horizon (since nothing can escape the event horizon in GR). The boundary conditions (ingoing at the event horizon and outgoing at infinity) select a discrete spectrum of complex frequencies ω (cf. the similar problem of the one-dimensional Schrodinger equation with a rectangular potential). The frequencies are known as “quasi-normal mode” (QNM) frequencies [65], and for non-extremal Kerr BHs they have strictly negative imaginary part, i.e., the modes that they describe are damped. These damped oscillations constitute the “ringdown” part of the GW signal from a BH binary.

From the procedure whereby they are derived, which we have just outlined, it is clear that for given multipole numbers ℓ, m , the QNM frequencies only depend (in GR) on the BH mass and spin. This is in a sense a consequence of the no-hair theorem of GR, which states that BHs can only be described by their mass and spin, and that they do not carry any additional “charges” or “hairs” [66]. (Note that BHs in GR can carry an electric charge, but for astrophysical BHs that is expected to be zero or negligible [67].)

The direct measurement of the QNM frequencies and decay times from the LIGO-Virgo detections is a difficult task because of the low SNR of the ringdown. Indeed, at present one can at most check the compatibility of the ringdown signal with the predictions of GR [3,11], i.e., with the QNM frequencies and decay times that would be expected based on the final remnant spin predicted via Equation (3) (or a similar method), once the masses and spin measurements from the inspiral part are factored in.

Stronger ringdown signals would allow not only for measuring, directly from the data, the frequency and decay time of the dominant, least damped QNM (the $\ell = m = 2$ mode for a quasicircular binary), but also the first subdominant mode (usually the $\ell = m = 3$ or $\ell = m = 4$, mode depending on the binary’s parameters). This would permit performing a null test of the no-hair theorem [68]. Indeed, as mentioned above, all QNM frequencies and decay times depend only on M and a in GR. Therefore, one could use the $\ell = m = 2$ measured frequency and decay time to infer M and a , use those to predict the frequency/decay time of the second QNM, and finally check the agreement with the measured value(s). This kind of test, however, would require not only that the ringdown signal be detectable (i.e., with SNR larger than ~ 8), but also that the SNR be sufficiently large to resolve both the dominant and first subdominant QNM. In practice, this requires an SNR of at least ~ 90 in the ringdown phase alone [57,69], which will be achieved routinely with LISA, but which will require

Voyager-type third-generation detectors on Earth [57] (unless one manages to stack several ringdown signals together by rescaling them [70]).

Several observations can be made at this stage. First, in theories of gravity extending GR, not only can the spin-2 QNMs differ from GR (as a result e.g., of BHs carrying hairs, or simply because of the different field equations at linear order [71]), but there may also be QNMs with different helicities (e.g., scalars, vectors, or even additional tensor modes in bimetric gravitational theories) [72]. These QNMs would give rise to different polarizations in the response of a network of GW detectors, and would be in principle distinguishable from purely spin-2 modes [73]. However, as mentioned previously, non-GR gravitons must be coupled very weakly to a detector (if coupled at all) to ensure the absence of unwanted fifth forces in experiments testing the (weak) equivalence principle on Earth. Therefore, the coupling of QNMs of helicity $s \neq \pm 2$ to the detector will be strongly suppressed (see, e.g., Ref. [59] for an explicit example).

Secondly, let us note that in the geometric optics limit (i.e., $\ell \gtrsim m \gg 1$) the equations of linear perturbation theory [Equation (8)] must reduce to the null geodesics equation. This is most easily seen by inserting the ansatz $\bar{h}_{\mu\nu} \approx A_{\mu\nu} \exp(iS)$ into Equation (4), and expanding in the limit of large $\partial_\mu S$ (i.e., in the limit of large frequencies and wavenumbers). This gives the null condition $g^{\mu\nu} \partial_\mu S \partial_\nu S = 0$, which coincides with the Hamilton-Jacobi equation for massless particles. From the derivative of this condition, one then obtains the null geodesics equation (cf., e.g., Section 7.8 of Ref. [74] for details). This result is of course hardly surprising as it simply amounts to saying that the gravitational wavefronts follow null geodesics (i.e., GWs travel at the speed of light), but it has noteworthy implications for the physics of QNMs. Indeed, since the linear perturbation equations must reduce to the null geodesics equation in the geometric optics limit, the potential V appearing in the QNM master equation (Equation (8)) must reduce to the effective potential governing the motion of null geodesics in Kerr in the limit $\ell \gtrsim m \gg 1$. In particular, in that limit the position of the peak of the potential must asymptote to the same location as the (unstable) circular photon orbit, and the frequencies of the QNMs are simply given by linear combinations of the orbital and frame-dragging precession frequencies of the circular photon orbit [75–77]. (Note that the frame-dragging precession frequency only appears in the QNM expressions for spinning BHs.) Moreover, one can show that the decay times of the QNMs for $\ell \gtrsim m \gg 1$ are related to the Lyapunov exponents of null geodesics near the circular photon orbit, which in turn depend on the curvature of the effective potential for null geodesics near its peak [75,76]. An intuitive interpretation of these results is that the QNMs are generated at the circular photon orbit and slowly leak outward, since that orbit is unstable to radial perturbations.

From this point of view, it is clear that the physics of the QNMs is very similar (if not the same) as that of the circular photon orbit, and electromagnetic experiments aiming to explore the latter present clear synergies with GW detectors. One example is given by the Event Horizon Telescope [78], an ongoing very long baseline radio interferometry experiment aiming to observe the near horizon region of Sgr A* (the massive BH at the center of our Galaxy), and which has recently provided the first “shadow image” of the horizon of the massive BH at the center of M87 [79]. Another implication of realizing that QNMs are generated near the circular photon orbit is that BH mimickers that deviate significantly from the Schwarzschild/Kerr geometry in that region may be severely constrained once GW interferometers detect the ringdown part of a binary’s signal with sufficiently large SNR.

5. The Post-Ringdown

From the derivation of the QNMs outlined in the previous section, it is clear that, if the boundary conditions at the event horizon are not perfectly ingoing, the QNM frequencies and decay times will in general change. Partially or fully reflective boundary conditions may in fact be physically relevant in case the merger remnant is not a BH but a more exotic horizonless object (e.g., a wormhole [18], or an ensemble of horizonless quantum states [80–86]), perhaps motivated by attempts to solve the information loss paradox [87]. Other possible deviations from the GR event horizon paradigm may arise in theories that violate Lorentz symmetry in the purely gravitational sector [28,88].

In the presence of such deviations from purely ingoing boundary conditions, part of the GW radiation generated at the peak of the potential (i.e., roughly at the circular photon orbit, where QNMs are produced) is reflected off the horizon. Part of this reflected radiation then tunnels through the potential barrier at the circular photon orbit (eventually reaching infinity), while the rest is reflected back again toward the horizon, where the process can restart. Therefore, after the ringdown described in the previous section, which corresponds to radiation generated at the potential's peak and leaking outward, there appears a series of “echoes” delayed (relative to the initial ringdown signal) by multiples of twice the light travel time between the circular photon orbit and the effective “mirror” at the horizon [67,89–92].

A similar phenomenon can take place in the presence of matter far away from the BH, which can act as a partially reflective mirror for outgoing radiation. Indeed, the matter's gravitational potential can give rise to a “bump” in the potential V appearing in Equation (8) [67,89]. In this case, after the initial ringdown “burst”, one would have echoes delayed by multiples of twice the light travel time between the circular photon orbit and the far away matter. An example from Ref. [89] is shown in Figure 1. As can be seen, the initial ringdown transient is governed by the QNM frequencies and decay times of the pure Kerr/Schwarzschild system (without any matter), while only after a delay of twice the light travel time between the circular photon orbit and the matter does the signal start to be described by the QNMs of the composite system. The same applies to the case of a BH mimicker with near horizon reflectivity [18,67,89]: the initial ringdown transient has spectrum comprised of the Kerr/Schwarzschild QNMs, while the “true” QNMs (accounting for the modified boundary conditions at the horizon) only become apparent after a time roughly equal to twice the light travel time between the near horizon mirror and the potential's peak.

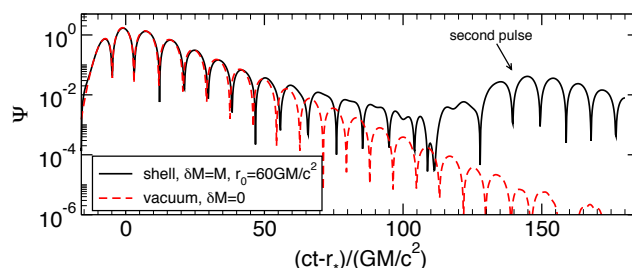


Figure 1. Axial waveform for a Gaussian pulse, scattered off a system comprised of a Schwarzschild BH and a thin shell located at $r_0 = 60 \text{ GM}/c^2$ and with mass equal to the BH mass M . The Gaussian pulse is initially placed near the ISCO, with width $\sigma = 4 \text{ GM}/c^2$. Note that the signal is initially dominated by the isolated BH QNMs, with the effect of matter appearing as a second pulse at later times. Adapted from Ref. [89].

The presence of echoes in the post-ringdown signal of some of the LIGO-Virgo systems was put forward by the authors of [93–95], but the claim is highly controversial as later analyses have found it to have low significance [96,97]. Such a low significance (if any) is not surprising since the systems detected by LIGO-Virgo have very small ringdown SNR. Nevertheless, third-generation ground-based detectors and LISA will allow for measuring the ringdown phase with much higher SNR [57], which could open the way to detecting echoes, if there are any.

A more robust way to assess the possible presence of echoes is to look at their interaction with BH spins. Energy conservation dictates that the echoes should have successively decreasing amplitude around a non-spinning BH, but their amplitude can actually increase around BHs with sufficiently large spins. This is due to a phenomenon called super-radiance [98–101], which is strictly related to the existence of an ergoregion (i.e., a near-horizon region where modes with negative energy can exist as seen by an observer at infinity), and whereby echoes can extract rotational energy from the spinning BH. Indeed, BHs with sufficiently large spins and surrounded by a “mirror” at the horizon become linearly unstable because of super-radiance, meaning that the QNMs of the system are not damped but

exponentially growing (at the expense of the BH’s rotational energy). This instability is also known as “BH bomb” instability [102,103], and if present would have important consequences for the background of unresolved GWs that LIGO and Virgo are trying to detect [104]. Indeed, if all astrophysical BH candidates in the universe (in binaries or isolated) had a perfectly reflective mirror at the horizon, or if they had no horizon at all and they let gravitational radiation go through them undamped, under reasonable assumptions on the distributions of their spins, their exponentially growing QNMs would sum up to create a stochastic background of GWs orders of magnitude larger than the current upper bounds from LIGO-Virgo [104]. This allows us to exclude that all BH candidates in the universe have a perfectly reflective horizon surface, or that they let gravitational radiation go through them undamped. Indeed, LIGO-Virgo at design sensitivity will only allow for 1% or less of the BH candidate population to have such properties. The constraint can be extended to partially reflective mirrors or to objects that damp passing radiation. However, a transmissivity—or energy loss through the object—of at least 60% (6%) can quench the instability for any spin (for spins $a \lesssim 0.9$), thus evading these constraints [104,105].

Let us note that a similar BH bomb super-radiant instability affects BHs with sufficiently large spins and a mirror at large distances from the BH [102,103]. Indeed, if this mirror has sufficiently large reflectivity, it can focus gravitational radiation back to the BH. This reflected radiation would in turn be scattered back by the effective potential of Equation (8), and so on. Since the ergoregion of Kerr BHs extends (on the equatorial plane) to $r = 2r_s$ in Boyer–Lindquist coordinates, while the circular photon orbit has radius that goes to r_s in the same coordinates for $a \rightarrow 1$ [38], it is clear that while bouncing back and forth between the potential’s peak and the mirror the wave can get amplified by producing negative energy ergoregion modes, as in the case of a mirror at the horizon.

While matter around the BH will not typically provide sufficient reflectivity for this instability to pick up, a physical implementation of this idea is provided by ultralight bosonic degrees of freedom. Indeed, such boson fields (be them scalar, vectors or tensors) can become super-radiance unstable around BHs with sufficiently large spin, provided that their Compton wavelength is comparable to the BH horizon radius [106]. The instability is akin to the BH bomb with an external mirror, where the mirror is provided here by the mass, which constrains the boson field near the BH by allowing for bosonic bound states. As a result of the instability, the BH spin quickly decreases, and the angular momentum is transferred to the boson field, which evolves into a rotating dipolar condensate. This condensate is in turn expected to emit almost monochromatic GWs, as can be understood simply from the quadrupole formula [107–113]. Summing up the monochromatic waves that would be produced by all the (isolated) BHs in the universe, under reasonable assumptions for their spins, one obtains a stochastic background of GWs that exceeds the current LIGO-Virgo bounds by several orders of magnitude if the boson’s mass is in the right range [114,115]. In more details, current LIGO-Virgo bounds on the stochastic background [116] exclude boson masses between roughly 2×10^{-13} eV and 10^{-12} eV [114,115]. Similarly, LISA will allow for ruling out masses in the range $\sim 5 \times [10^{-19}, 10^{-16}]$ eV [114,115]. Further constraints may come from trying to detect the monochromatic GWs produced by the bosonic condensate directly, either in isolated BHs, or in the remnant resulting from a BH merger [108,113–115,117–120].

6. Conclusions

In this pedagogical note, I have tried to show how the GW signal from the merger of two BHs can be understood qualitatively based on very simple physical ingredients, including the quadrupole formula, which allows for understanding the low frequency inspiral and its dependence on the chirp mass; the PN precession of the spins during the inspiral; the presence of an effective ISCO, whose position depends on the BH spins as a result of “frame dragging” and which affects the overall power emitted in GWs; and the circular photon orbit and its effective potential, whose physics determines the QNMs. I have also shown how modifications of GR and/or of the BH paradigm can affect each of these ingredients and produce GW signals differing from GR. In particular, I have briefly outlined low frequency modifications to the gravitational waveform that may arise from BH dipole radiation

(caused in turn by BH hairs); possible changes to the conservative dynamics, which may result in changes of the ISCO properties and therefore in a different final spin; changes in the physics of the circular photon orbit, which would affect the properties of QNMs; and changes in the boundary conditions satisfied by the QNMs at the horizon and at infinity (as a result of exotic near horizon physics, matter far from the binary, or the presence of an ultralight boson field), which would result in echoes and super-radiant instabilities.

Funding: This work received funding from the European Research Council (ERC) under the European Union’s Horizon 2020 research and innovation programme (grant agreement no. GRAMS-815673; project title “GRavity from Astrophysical to Microscopic Scales”). This work was also supported by the H2020-MSCA-RISE-2015 Grant No. StronGrHEP-690904. The author would like to acknowledge networking support by the COST Action CA16104.

Conflicts of Interest: The author declares no conflict of interest.

References

1. Abbott, B.P.; Abbott, R.; Abbott, T.D.; Abernathy, M.R.; Acernese, F.; Ackley, K.; Adams, C.; Adams, T.; Addesso, P.; Adhikari, R.X.; et al. Observation of Gravitational Waves from a Binary Black Hole Merger. *Phys. Rev. Lett.* **2016**, *116*, 061102. doi:10.1103/PhysRevLett.116.061102.
2. Abbott, B.P.; Abbott, R.; Abbott, T.D.; Abernathy, M.R.; Acernese, F.; Ackley, K.; Adams, C.; Adams, T.; Addesso, P.; Adhikari, R.X.; et al. GW151226: Observation of Gravitational Waves from a 22-Solar-Mass Binary Black Hole Coalescence. *Phys. Rev. Lett.* **2016**, *116*, 241103, doi:10.1103/PhysRevLett.116.241103.
3. Abbott, B.P.; Abbott, R.; Abbott, T.D.; Abernathy, M.R.; Acernese, F.; Ackley, K.; Adams, C.; Adams, T.; Addesso, P.; Adhikari, R.X.; et al. Binary Black Hole Mergers in the first Advanced LIGO Observing Run. *Phys. Rev. X* **2016**, *6*, 041015, doi:10.1103/PhysRevX.6.041015, 10.1103/PhysRevX.8.039903.
4. Scientific, L.I.; Abbott, B.P.; Abbott, R.; Abbott, T.D.; Acernese, F.; Ackley, K.; Adams, C.; Adams, T.; Addesso, P.; Adhikari, R.X.; et al. GW170104: Observation of a 50-Solar-Mass Binary Black Hole Coalescence at Redshift 0.2. *Phys. Rev. Lett.* **2017**, *118*, 221101, doi:10.1103/PhysRevLett.118.221101, 10.1103/PhysRevLett.121.129901.
5. Abbott, B.P.; Abbott, R.; Abbott, T.D.; Acernese, F.; Ackley, K.; Adams, C.; Adams, T.; Addesso, P.; Adhikari, R.X.; Adya, V.B.; et al. GW170608: Observation of a 19-solar-mass Binary Black Hole Coalescence. *Astrophys. J.* **2017**, *851*, L35, doi:10.3847/2041-8213/aa9f0c.
6. Abbott, B.P.; Abbott, R.; Abbott, T.D.; Acernese, F.; Ackley, K.; Adams, C.; Adams, T.; Addesso, P.; Adhikari, R.X.; Adya, V.B.; et al. GW170814: A Three-Detector Observation of Gravitational Waves from a Binary Black Hole Coalescence. *Phys. Rev. Lett.* **2017**, *119*, 141101, doi:10.1103/PhysRevLett.119.141101.
7. Abbott, B.P.; Abbott, R.; Abbott, T.D.; Acernese, F.; Ackley, K.; Adams, C.; Adams, T.; Addesso, P.; Adhikari, R.X.; Adya, V.B.; et al. GWTC-1: A Gravitational-Wave Transient Catalog of Compact Binary Mergers Observed by LIGO and Virgo during the First and Second Observing Runs. *arXiv* **2018**, arXiv:1811.12907.
8. Will, C.M. The Confrontation between General Relativity and Experiment. *Living Rev. Relativ.* **2014**, *17*, 4, doi:10.12942/lrr-2014-4.
9. Hulse, R.A.; Taylor, J.H. Discovery of a pulsar in a binary system. *Astrophys. J.* **1975**, *195*, L51–L53, doi:10.1086/181708.
10. Damour, T.; Taylor, J.H. Strong field tests of relativistic gravity and binary pulsars. *Phys. Rev. D* **1992**, *45*, 1840–1868, doi:10.1103/PhysRevD.45.1840.
11. Abbott, B.P.; Abbott, R.; Abbott, T.D.; Abernathy, M.R.; Acernese, F.; Ackley, K.; Adams, C.; Adams, T.; Addesso, P.; Adhikari, R.X.; et al. Tests of general relativity with GW150914. *Phys. Rev. Lett.* **2016**, *116*, 221101, doi:10.1103/PhysRevLett.116.221101.
12. Peters, P.C. Gravitational Radiation and the Motion of Two Point Masses. *Phys. Rev.* **1964**, *136*, B1224–B1232, doi:10.1103/PhysRev.136.B1224.
13. Blanchet, L. Gravitational Radiation from Post-Newtonian Sources and Inspiralling Compact Binaries. *Living Rev. Relativ.* **2014**, *17*, 2, doi:10.12942/lrr-2014-2.

14. Apostolatos, T.A.; Cutler, C.; Sussman, G.S.; Thorne, K.S. Spin-induced orbital precession and its modulation of the gravitational waveforms from merging binaries. *Phys. Rev. D* **1994**, *49*, 6274, doi:10.1103/PhysRevD.49.6274.
15. Barausse, E.; Rezzolla, L. Predicting the direction of the final spin from the coalescence of two black holes. *Astrophys. J.* **2009**, *704*, L40–L44, doi:10.1088/0004-637X/704/1/L40.
16. Amaro-Seoane, P.; Audley, H.; Babak, S.; Baker, J.; Barausse, E.; Bender, P.; Berti, E.; Binetruy, P.; Born, M.; Bortoluzzi, D.; et al. Laser Interferometer Space Antenna. *arXiv* **2017**, arXiv:1702.00786.
17. Klein, A.; Barausse, E.; Sesana, A.; Petiteau, A.; Berti, E.; Babak, S.; Gair, J.; Aoudia, S.; Hinder, I.; Ohme, F.; et al. Science with the space-based interferometer eLISA: Supermassive black hole binaries. *Phys. Rev. D* **2016**, *93*, 024003, doi:10.1103/PhysRevD.93.024003.
18. Cardoso, V.; Franzin, E.; Maselli, A.; Pani, P.; Raposo, G. Testing strong-field gravity with tidal Love numbers. *Phys. Rev. D* **2017**, *95*, 084014.
19. Barausse, E.; Yunes, N.; Chamberlain, K. Theory-Agnostic Constraints on Black-Hole Dipole Radiation with Multiband Gravitational-Wave Astrophysics. *Phys. Rev. Lett.* **2016**, *116*, 241104, doi:10.1103/PhysRevLett.116.241104.
20. Eardley, D.M. Observable effects of a scalar gravitational field in a binary pulsar. *Astrophys. J. Lett.* **1975**, *196*, L59–L62, doi:10.1086/181744.
21. Nordtvedt, K. Equivalence Principle for Massive Bodies. I. Phenomenology. *Phys. Rev.* **1968**, *169*, 1014–1016, doi:10.1103/PhysRev.169.1014.
22. Nordtvedt, K. Equivalence Principle for Massive Bodies. 2. Theory. *Phys. Rev.* **1968**, *169*, 1017–1025.
23. Damour, T.; Esposito-Farese, G. Tensor-multi-scalar theories of gravitation. *Class. Quantum Gravity* **1992**, *9*, 2093.
24. Will, C.M.; Zaglauer, H.W. Gravitational Radiation, Close Binary Systems, and the Brans-dicke Theory of Gravity. *Astrophys. J.* **1989**, *346*, 366, doi:10.1086/168016.
25. Foster, B.Z. Strong field effects on binary systems in Einstein-aether theory. *Phys. Rev. D* **2007**, *76*, 084033, doi:10.1103/PhysRevD.76.084033.
26. Yagi, K.; Blas, D.; Yunes, N.; Barausse, E. Strong Binary Pulsar Constraints on Lorentz Violation in Gravity. *Phys. Rev. Lett.* **2014**, *112*, 161101, doi:10.1103/PhysRevLett.112.161101.
27. Yagi, K.; Blas, D.; Barausse, E.; Yunes, N. Constraints on Einstein-aether theory and Hořava gravity from binary pulsar observations. *Phys. Rev. D* **2014**, *89*, 084067.
28. Ramos, O.; Barausse, E. Constraints on Horava gravity from binary black hole observations. *Phys. Rev. D* **2019**, *99*, 024034, doi:10.1103/PhysRevD.99.024034.
29. Shao, L.; Sennett, N.; Buonanno, A.; Kramer, M.; Wex, N. Constraining nonperturbative strong-field effects in scalar-tensor gravity by combining pulsar timing and laser-interferometer gravitational-wave detectors. *Phys. Rev. X* **2017**, *7*, 041025, doi:10.1103/PhysRevX.7.041025.
30. Barausse, E.; Yagi, K. Gravitation-Wave Emission in Shift-Symmetric Horndeski Theories. *Phys. Rev. Lett.* **2015**, *115*, 211105, doi:10.1103/PhysRevLett.115.211105.
31. Yagi, K.; Stein, L.C.; Yunes, N. Challenging the Presence of Scalar Charge and Dipolar Radiation in Binary Pulsars. *Phys. Rev. D* **2016**, *93*, 024010, doi:10.1103/PhysRevD.93.024010.
32. Sesana, A. Prospects for Multiband Gravitational-Wave Astronomy after GW150914. *Phys. Rev. Lett.* **2016**, *116*, 231102, doi:10.1103/PhysRevLett.116.231102.
33. Babak, S.; Gair, J.; Sesana, A.; Barausse, E.; Sopuerta, C.F.; Berry, C.P.L.; Berti, E.; Amaro-Seoane, P.; Petiteau, A.; Klein, A. Science with the space-based interferometer LISA. V. Extreme mass-ratio inspirals. *Phys. Rev. D* **2017**, *95*, 103012, doi:10.1103/PhysRevD.95.103012.
34. Misner, C.W.; Thorne, K.S.; Wheeler, J.A. *Gravitation*; W. H. Freeman: San Francisco, CA, USA, 1973.
35. Le Tiec, A.; Barausse, E.; Buonanno, A. Gravitational Self-Force Correction to the Binding Energy of Compact Binary Systems. *Phys. Rev. Lett.* **2012**, *108*, 131103, doi:10.1103/PhysRevLett.108.131103.
36. Barack, L.; Sago, N. Gravitational self-force correction to the innermost stable circular orbit of a Schwarzschild black hole. *Phys. Rev. Lett.* **2009**, *102*, 191101, doi:10.1103/PhysRevLett.102.191101.
37. Buonanno, A.; Chen, Y.B.; Vallisneri, M. Detecting gravitational waves from precessing binaries of spinning compact objects: Adiabatic limit. *Phys. Rev. D* **2003**, *67*, 104025.
38. Bardeen, J.M.; Press, W.H.; Teukolsky, S.A. Rotating black holes: Locally nonrotating frames, energy extraction, and scalar synchrotron radiation. *Astrophys. J.* **1972**, *178*, 347, doi:10.1086/151796.

39. Middleton, M. Black hole spin: Theory and observation. In *Astrophysics of Black Holes*; Springer: Berlin/Heidelberg, Germany, 2016; pp. 99–151.
40. Brenneman, L. Measuring Supermassive Black Hole Spins in Active Galactic Nuclei. *arXiv* **2013**, arXiv:1309.6334.
41. Bambi, C.; Barausse, E. Constraining the quadrupole moment of stellar-mass black-hole candidates with the continuum fitting method. *Astrophys. J.* **2011**, *731*, 121, doi:10.1088/0004-637X/731/2/121.
42. Bambi, C.; Barausse, E. The Final stages of accretion onto non-Kerr compact objects. *Phys. Rev. D* **2011**, *84*, 084034, doi:10.1103/PhysRevD.84.084034.
43. Campanelli, M.; Lousto, C.O.; Zlochower, Y. Spinning-black-hole binaries: The orbital hang up. *Phys. Rev. D* **2006**, *74*, 041501, doi:10.1103/PhysRevD.74.041501.
44. Barausse, E.; Morozova, V.; Rezzolla, L. On the mass radiated by coalescing black-hole binaries. *Astrophys. J.* **2012**, *758*, 63.
45. Kesden, M. Can binary mergers produce maximally spinning black holes? *Phys. Rev. D* **2008**, *78*, 084030, doi:10.1103/PhysRevD.78.084030.
46. Scheel, M.A.; Boyle, M.; Chu, T.; Kidder, L.E.; Matthews, K.D.; Pfeiffer, H.P. High-accuracy waveforms for binary black hole inspiral, merger, and ringdown. *Phys. Rev. D* **2009**, *79*, 024003, doi:10.1103/PhysRevD.79.024003.
47. Buonanno, A.; Kidder, L.E.; Lehner, L. Estimating the final spin of a binary black hole coalescence. *Phys. Rev. D* **2008**, *77*, 026004, doi:10.1103/PhysRevD.77.026004.
48. Rezzolla, L.; Barausse, E.; Dorband, E.N.; Pollney, D.; Reisswig, C.; Seiler, J.; Husa, S. On the final spin from the coalescence of two black holes. *Phys. Rev. D* **2008**, *78*, 044002, doi:10.1103/PhysRevD.78.044002.
49. Hofmann, F.; Barausse, E.; Rezzolla, L. The final spin from binary black holes in quasi-circular orbits. *Astrophys. J.* **2016**, *825*, L19, doi:10.3847/2041-8205/825/2/L19.
50. Healy, J.; Lousto, C.O. Hangup effect in unequal mass binary black hole mergers and further studies of their gravitational radiation and remnant properties. *Phys. Rev. D* **2018**, *97*, 084002, doi:10.1103/PhysRevD.97.084002.
51. Varma, V.; Gerosa, D.; Stein, L.C.; Hebert, F.; Zhang, H. High-accuracy mass, spin, and recoil predictions of generic black-hole merger remnants. *Phys. Rev. Lett.* **2019**, *122*, 011101, doi:10.1103/PhysRevLett.122.011101.
52. Brezin, E.; Itzykson, C.; Zinn-Justin, J. Relativistic Balmer Formula Including Recoil Effects. *Phys. Rev. D* **1970**, *1*, 2349–2355, doi:10.1103/PhysRevD.1.2349.
53. Buonanno, A.; Damour, T. Effective one-body approach to general relativistic two-body dynamics. *Phys. Rev. D* **1999**, *59*, 084006, doi:10.1103/PhysRevD.59.084006.
54. Damour, T.; Jaranowski, P.; Schaefer, G. Effective one body approach to the dynamics of two spinning black holes with next-to-leading order spin-orbit coupling. *Phys. Rev. D* **2008**, *78*, 024009, doi:10.1103/PhysRevD.78.024009.
55. Barausse, E.; Buonanno, A. An Improved effective-one-body Hamiltonian for spinning black-hole binaries. *Phys. Rev. D* **2010**, *81*, 084024, doi:10.1103/PhysRevD.81.084024.
56. Babak, S.; Taracchini, A.; Buonanno, A. Validating the effective-one-body model of spinning, precessing binary black holes against numerical relativity. *Phys. Rev. D* **2017**, *95*, 024010, doi:10.1103/PhysRevD.95.024010.
57. Berti, E.; Sesana, A.; Barausse, E.; Cardoso, V.; Belczynski, K. Spectroscopy of Kerr black holes with Earth- and space-based interferometers. *Phys. Rev. Lett.* **2016**, *117*, 101102, doi:10.1103/PhysRevLett.117.101102.
58. Abuter, R.; Amorim, A.; Anugu, N.; Bauböck, M.; Benisty, M.; Berger, J.P.; Blind, N.; Bonnet, H.; Brner, W.; Buron, A.; et al. Detection of the gravitational redshift in the orbit of the star S2 near the Galactic centre massive black hole. *Astron. Astrophys.* **2018**, *615*, L15, doi:10.1051/0004-6361/201833718.
59. Barausse, E.; Palenzuela, C.; Ponce, M.; Lehner, L. Neutron-star mergers in scalar-tensor theories of gravity. *Phys. Rev. D* **2013**, *87*, 081506, doi:10.1103/PhysRevD.87.081506.
60. Palenzuela, C.; Barausse, E.; Ponce, M.; Lehner, L. Dynamical scalarization of neutron stars in scalar-tensor gravity theories. *Phys. Rev. D* **2014**, *89*, 044024, doi:10.1103/PhysRevD.89.044024.
61. Pfennig, M.J.; Poisson, E. Scalar, electromagnetic, and gravitational selfforces in weakly curved space-times. *Phys. Rev. D* **2002**, *65*, 084001, doi:10.1103/PhysRevD.65.084001.
62. Sciama, D.W.; Waylen, P.C.; Gilman, R.C. Generally covariant integral formulation of einstein's field equation. *Phys. Rev.* **1969**, *187*, 1762–1766, doi:10.1103/PhysRev.187.1762.

63. Newman, E.; Penrose, R. An Approach to gravitational radiation by a method of spin coefficients. *J. Math. Phys.* **1962**, *3*, 566–578, doi:10.1063/1.1724257.
64. Teukolsky, S.A. Perturbations of a rotating black hole. 1. Fundamental equations for gravitational electromagnetic and neutrino field perturbations. *Astrophys. J.* **1973**, *185*, 635–647, doi:10.1086/152444.
65. Berti, E.; Cardoso, V.; Starinets, A.O. Quasinormal modes of black holes and black branes. *Class. Quantum Gravity* **2009**, *26*, 163001, doi:10.1088/0264-9381/26/16/163001.
66. Carter, B. Axisymmetric Black Hole has only Two Degrees of Freedom. *Phys. Rev. Lett.* **1971**, *26*, 331–333, doi:10.1103/PhysRevLett.26.331.
67. Barausse, E.; Cardoso, V.; Pani, P. Can environmental effects spoil precision gravitational-wave astrophysics? *Phys. Rev. D* **2014**, *89*, 104059, doi:10.1103/PhysRevD.89.104059.
68. Dreyer, O.; Kelly, B.J.; Krishnan, B.; Finn, L.S.; Garrison, D.; Lopez-Aleman, R. Black hole spectroscopy: Testing general relativity through gravitational wave observations. *Class. Quantum Gravity* **2004**, *21*, 787–804, doi:10.1088/0264-9381/21/4/003.
69. Berti, E.; Cardoso, J.; Cardoso, V.; Cavaglia, M. Matched-filtering and parameter estimation of ringdown waveforms. *Phys. Rev. D* **2007**, *76*, 104044, doi:10.1103/PhysRevD.76.104044.
70. Yang, H.; Paschalidis, V.; Yagi, K.; Lehner, L.; Pretorius, F.; Yunes, N. Gravitational wave spectroscopy of binary neutron star merger remnants with mode stacking. *Phys. Rev. D* **2018**, *97*, 024049, doi:10.1103/PhysRevD.97.024049.
71. Barausse, E.; Sotiriou, T.P. Perturbed Kerr Black Holes can probe deviations from General Relativity. *Phys. Rev. Lett.* **2008**, *101*, 099001, doi:10.1103/PhysRevLett.101.099001.
72. Berti, E.; Barausse, E.; Cardoso, V.; Gualtieri, L.; Pani, P.; Sperhake, U.; Stein, L.C.; Wex, N.; Yagi, K.; Baker, T.; et al. Testing General Relativity with Present and Future Astrophysical Observations. *Class. Quantum Gravity* **2015**, *32*, 243001, doi:10.1088/0264-9381/32/24/243001.
73. Eardley, D.M.; Lee, D.L.; Lightman, A.P.; Wagoner, R.V.; Will, C.M. Gravitational-Wave Observations as a Tool for Testing Relativistic Gravity. *Phys. Rev. Lett.* **1973**, *30*, 884–886, doi:10.1103/PhysRevLett.30.884.
74. de Felice, F.; Clarke, C.J.S. *Relativity on Curved Manifolds*; Cambridge University Press: Cambridge, UK, 1992.
75. Ferrari, V.; Mashhoon, B. New approach to the quasinormal modes of a black hole. *Phys. Rev. D* **1984**, *30*, 295–304, doi:10.1103/PhysRevD.30.295.
76. Schutz, B.F.; Will, C.M. Black hole normal modes—A semianalytic approach. *Astrophys. J. Lett.* **1985**, *291*, L33–L36, doi:10.1086/184453.
77. Yang, H.; Nichols, D.A.; Zhang, F.; Zimmerman, A.; Zhang, Z.; Chen, Y. Quasinormal-mode spectrum of Kerr black holes and its geometric interpretation. *Phys. Rev. D* **2012**, *86*, 104006, doi:10.1103/PhysRevD.86.104006.
78. Broderick, A.E.; Johannsen, T.; Loeb, A.; Psaltis, D. Testing the No-Hair Theorem with Event Horizon Telescope Observations of Sagittarius A*. *Astrophys. J.* **2014**, *784*, 7, doi:10.1088/0004-637X/784/1/7.
79. Event Horizon Telescope Collaboration; Akiyama, K.; Alberdi, A.; Alef, W.; Asada, K.; Azulay, R.; Baczkowski, A.K.; Ball, D.; Baloković, M.; Barrett, J.; et al. First M87 Event Horizon Telescope Results. I. The Shadow of the Supermassive Black Hole. *Astrophys. J. Lett.* **2019**, *875*, L1, doi:10.3847/2041-8213/ab0ec7.
80. Mazur, P.O.; Mottola, E. Gravitational vacuum condensate stars. *Proc. Natl. Acad. Sci. USA* **2004**, *101*, 9545–9550, doi:10.1073/pnas.0402717101.
81. Mathur, S.D. The Fuzzball proposal for black holes: An Elementary review. *Fortsch. Phys.* **2005**, *53*, 793–827, doi:10.1002/prop.200410203.
82. Mathur, S.D. Fuzzballs and the information paradox: A Summary and conjectures. *Adv. Sci. Lett.* **2009**, *2*, 133–150.
83. Barceló, C.; Carballo-Rubio, R.; Garay, L.J. Where does the physics of extreme gravitational collapse reside? *Universe* **2016**, *2*, 7, doi:10.3390/universe2020007.
84. Danielsson, U.H.; Dibitetto, G.; Giri, S. Black holes as bubbles of AdS. *J. High Energy Phys.* **2017**, *10*, 171, doi:10.1007/JHEP10(2017)171.
85. Berthiere, C.; Sarkar, D.; Solodukhin, S.N. The quantum fate of black hole horizons. *arXiv* **2017**, arXiv:1712.09914.
86. Cardoso, V.; Pani, P. The observational evidence for horizons: From echoes to precision gravitational-wave physics. *arXiv* **2017**, arXiv:1707.03021.
87. Almheiri, A.; Marolf, D.; Polchinski, J.; Sully, J. Black Holes: Complementarity or Firewalls? *J. High Energy Phys.* **2013**, *2*, 062, doi:10.1007/JHEP02(2013)062.

88. Blas, D.; Sibiryakov, S. Horava gravity versus thermodynamics: The Black hole case. *Phys. Rev. D* **2011**, *84*, 124043, doi:10.1103/PhysRevD.84.124043.
89. Barausse, E.; Cardoso, V.; Pani, P. Environmental Effects for Gravitational-wave Astrophysics. *J. Phys. Conf. Ser.* **2015**, *610*, 012044, doi:10.1088/1742-6596/610/1/012044.
90. Cardoso, V.; Franzin, E.; Pani, P. Is the gravitational-wave ringdown a probe of the event horizon? *Phys. Rev. Lett.* **2016**, *116*, 171101.
91. Cardoso, V.; Hopper, S.; Macedo, C.F.B.; Palenzuela, C.; Pani, P. Gravitational-wave signatures of exotic compact objects and of quantum corrections at the horizon scale. *Phys. Rev. D* **2016**, *94*, 084031, doi:10.1103/PhysRevD.94.084031.
92. Cardoso, V.; Pani, P. Tests for the existence of horizons through gravitational wave echoes. *Nat. Astron.* **2017**, *1*, 586–591, doi:10.1038/s41550-017-0225-y.
93. Abedi, J.; Dykaar, H.; Afshordi, N. Echoes from the Abyss: The Holiday Edition! *arXiv* **2017**, arXiv:1701.03485.
94. Abedi, J.; Afshordi, N. Echoes from the Abyss: A highly spinning black hole remnant for the binary neutron star merger GW170817. *arXiv* **2018**, arXiv:1803.10454.
95. Abedi, J.; Dykaar, H.; Afshordi, N. Comment on: “Low significance of evidence for black hole echoes in gravitational wave data”. *arXiv* **2018**, arXiv:1803.08565.
96. Westerweck, J.; Nielsen, A.; Fischer-Birnholtz, O.; Cabero, M.; Capano, C.; Dent, T.; Krishnan, B.; Meadors, G.; Nitz, A.H. Low significance of evidence for black hole echoes in gravitational wave data. *Phys. Rev. D* **2018**, *97*, 124037, doi:10.1103/PhysRevD.97.124037.
97. Nielsen, A.B.; Capano, C.D.; Birnholtz, O.; Westerweck, J. Parameter estimation and statistical significance of echoes following black hole signals in the first Advanced LIGO observing run. *Phys. Rev. D* **2019**, *99*, 104012, doi:10.1103/PhysRevD.99.104012.
98. Penrose, R. Gravitational collapse: The role of general relativity. *La Rivista del Nuovo Cimento* **1969**, *1*, 252–276.
99. Zel’dovich, Y.B. GENERATION OF WAVES BY A ROTATION BODY. Available online: http://www.jetpletters.ac.ru/ps/1604/article_24607.pdf (accessed on 12 June 2019).
100. Zel’dovich, Y.B. Amplification of Cylindrical Electromagnetic Waves Reflected from a Rotating Body. Available online: <http://www.jetp.ac.ru/cgi-bin/e/index/e/35/6/p1085?a=list> (accessed on 12 June 2019).
101. Brito, R.; Cardoso, V.; Pani, P. Superradiance. *Lect. Notes Phys.* **2015**, *906*, 1–237, doi:10.1007/978-3-319-19000-6.
102. Press, W.H.; Teukolsky, S.A. Floating Orbits, Superradiant Scattering and the Black-hole Bomb. *Nature* **1972**, *238*, 211–212, doi:10.1038/238211a0.
103. Cardoso, V.; Dias, O.J.C.; Lemos, J.P.S.; Yoshida, S. The black hole bomb and superradiant instabilities. *Phys. Rev. D* **2004**, *70*, 044039, doi:10.1103/PhysRevD.70.044039.
104. Barausse, E.; Brito, R.; Cardoso, V.; Dvorkin, I.; Pani, P. The stochastic gravitational-wave background in the absence of horizons. *Class. Quantum Gravity* **2018**, *35*, 20LT01, doi:10.1088/1361-6382/aae1de.
105. Maggio, E.; Cardoso, V.; Dolan, S.R.; Pani, P. Ergoregion instability of exotic compact objects: Electromagnetic and gravitational perturbations and the role of absorption. *Phys. Rev. D* **2019**, *99*, 064007.
106. Detweiler, S.L. Klein-Gordon Equation and Rotating Black Holes. *Phys. Rev. D* **1980**, *22*, 2323–2326, doi:10.1103/PhysRevD.22.2323.
107. Yoshino, H.; Kodama, H. Gravitational radiation from an axion cloud around a black hole: Superradiant phase. *Prog. Theor. Exp. Phys.* **2014**, *2014*, 043E02, doi:10.1093/ptep/ptu029.
108. Brito, R.; Cardoso, V.; Pani, P. Black holes as particle detectors: Evolution of superradiant instabilities. *Class. Quantum Gravity* **2015**, *32*, 134001, doi:10.1088/0264-9381/32/13/134001.
109. East, W.E.; Pretorius, F. Superradiant Instability and Backreaction of Massive Vector Fields around Kerr Black Holes. *Phys. Rev. Lett.* **2017**, *119*, 041101, doi:10.1103/PhysRevLett.119.041101.
110. East, W.E. Superradiant instability of massive vector fields around spinning black holes in the relativistic regime. *Phys. Rev. D* **2017**, *96*, 024004, doi:10.1103/PhysRevD.96.024004.
111. Pani, P.; Cardoso, V.; Gualtieri, L.; Berti, E.; Ishibashi, A. Black hole bombs and photon mass bounds. *Phys. Rev. Lett.* **2012**, *109*, 131102, doi:10.1103/PhysRevLett.109.131102.
112. Pani, P.; Cardoso, V.; Gualtieri, L.; Berti, E.; Ishibashi, A. Perturbations of slowly rotating black holes: Massive vector fields in the Kerr metric. *Phys. Rev. D* **2012**, *86*, 104017, doi:10.1103/PhysRevD.86.104017.
113. Baryakhtar, M.; Lasenby, R.; Teo, M. Black Hole Superradiance Signatures of Ultralight Vectors. *Phys. Rev. D* **2017**, *96*, 035019.

114. Brito, R.; Ghosh, S.; Barausse, E.; Berti, E.; Cardoso, V.; Dvorkin, I.; Klein, A.; Pani, P. Gravitational wave searches for ultralight bosons with LIGO and LISA. *Phys. Rev. D* **2017**, *96*, 064050, doi:10.1103/PhysRevD.96.064050.
115. Brito, R.; Ghosh, S.; Barausse, E.; Berti, E.; Cardoso, V.; Dvorkin, I.; Klein, A.; Pani, P. Stochastic and resolvable gravitational waves from ultralight bosons. *Phys. Rev. Lett.* **2017**, *119*, 131101, doi:10.1103/PhysRevLett.119.131101.
116. Abbott, B.P.; Abbott, R.; Abbott, T.D.; Abernathy, M.R.; Acernese, F.; Ackley, K.; Adams, C.; Adams, T.; Addesso, P.; Adhikari, R.X.; et al. GW150914: Implications for the stochastic gravitational wave background from binary black holes. *Phys. Rev. Lett.* **2016**, *116*, 131102, doi:10.1103/PhysRevLett.116.131102.
117. Arvanitaki, A.; Dubovsky, S. Exploring the String Axiverse with Precision Black Hole Physics. *Phys. Rev. D* **2011**, *83*, 044026, doi:10.1103/PhysRevD.83.044026.
118. Arvanitaki, A.; Baryakhtar, M.; Huang, X. Discovering the QCD Axion with Black Holes and Gravitational Waves. *Phys. Rev. D* **2015**, *91*, 084011, doi:10.1103/PhysRevD.91.084011.
119. Arvanitaki, A.; Baryakhtar, M.; Dimopoulos, S.; Dubovsky, S.; Lasenby, R. Black Hole Mergers and the QCD Axion at Advanced LIGO. *Phys. Rev. D* **2017**, *95*, 043001, doi:10.1103/PhysRevD.95.043001.
120. Dev, P.S.B.; Lindner, M.; Ohmer, S. Gravitational Waves as a New Probe of Bose-Einstein Condensate Dark Matter. *Phys. Lett. B* **2017**, *773*, 219–224.



© 2019 by the authors. Licensee MDPI, Basel, Switzerland. This article is an open access article distributed under the terms and conditions of the Creative Commons Attribution (CC BY) license (<http://creativecommons.org/licenses/by/4.0/>).